Proc. Natl. Acad. Sci. USA
Vol. 92, pp. 10074–10078, October 1995
Biophysics

Direct structure analysis in protein electron crystallography: Crystallographic phases for halorhodopsin to 6-Å resolution

(electron diffraction/crystal structure analysis/membrane proteins)

DOUGLAS L. DORSET

Electron Diffraction Department, Hauptman–Woodward Medical Research Institute, Inc., 73 High Street, Buffalo, NY 14203-1196

Communicated by Herbert A. Hauptman, Hauptman–Woodward Medical Research Institute, Buffalo, NY, July 14, 1995 (received for review April 19, 1995)

ABSTRACT **The crystal structure of halorhodopsin was determined in (centrosymmetric) projection to 6-Å resolution by direct methods that use only the amplitudes of the electron diffraction pattern. A multisolution technique was used to generate initial 15-Å-resolution basis sets, and after selection of the best phase set (by the closest match of $|E_{obs}|$ and $|E_{calc}|$), annealing of individual reflections was used to improve its accuracy. The Sayre equation was then used to expand the phase terms to 10 Å, followed again by phase annealing. A final expansion with the Sayre equation enlarged this corrected phase set to 6 Å. When the condition of density flatness was used to locate the best phase solution after each extension, a final structure could be observed that was quite similar to the one found earlier by analysis of electron micrographs.**

Electron crystallography has become a useful alternative to x-ray crystallography for determining the structures of proteins that crystallize only in thin layers (1, 2). A significant example is the class of integral membrane proteins that can be formed as two-dimensional crystalline sheets after reconstitution in a suitable phospholipid bilayer (3) (or, in some instances, as obtained from a natural membrane source). Such studies take advantage of the enhanced scattering cross-section of matter for electrons, thus permitting the study of individual microcrystalline samples. High-resolution studies (e.g., to 3.5 Å) have been reported for three classes of membrane protein (4–6), and, in one case, a close match could be made to an x-ray crystal structure determined independently from material crystallized with detergent (6, 7).

One of the salient advantages of electron crystallography is that it is an optical technique. That is to say, electron micrographs taken from frozen-hydrated or sugar-embedded samples can be used directly as a source of crystallographic phases to combine with the electron diffraction amplitudes, as outlined by Henderson *et al.* (8). The difficulty of obtaining this phase information increases with resolution, however, due to the need to define accurately the transfer function of the electron microscope objective lens, the destruction of the sample induced by radiation damage, and the loss of strict packing order due to paracrystalline distortions. While measures have been devised to correct for these perturbations, it would, perhaps, be convenient to start with the very accurate phase set obtained most easily from lower-resolution electron micrographs and then extend these directly to the higher resolution found in readily recorded electron diffraction patterns. Alternatively, it might even be possible to attempt a true *ab initio* phase determination based only on the diffraction amplitudes.

The first stated goal of phase extension from a lower-resolution set from an image has already been realized. Gilmore *et al.* (9) pioneered this effort with the use of maximum entropy and likelihood methods to extend 15-Å phase information from bacteriorhodopsin (8) to the 3.5-Å resolution of the electron diffraction pattern. A potential map very similar to the one depicted earlier by Henderson *et al.* (8), after an extensive analysis of electron micrographs, was obtained. More recently, satisfactory results (10, 11) also have been obtained for bacteriorhodopsin, halorhodopsin, and the *Escherichia coli* Omp F porin with the Sayre equation. In these studies, the suitability of various resolution domains to be correctly analyzed by direct phase extension also was evaluated to provide strategies for the determination of unknown structures.

There is still much work to be done in the solution of macromolecular crystal structures solely from diffraction amplitudes. Given atomic resolution diffraction data, direct analyses of small protein structures have become more frequent recently in x-ray crystallography (12–14), principally due to the design of analytical techniques such as the "Shake and Bake" algorithm utilizing the minimal principle (14) as a figure of merit. Actual *ab initio* phase determinations of lower-resolution data sets, given no other phase information, are virtually unknown, however, although some progress has been made in the use of "glob" models to search for a starting low-resolution phase set (15). To promote further development of this important research area, the following work describes the procedure used to solve the structure of a centrosymmetric zone for halorhodopsin, based only on the reported electron diffraction amplitudes measured to 6-Å resolution.

ANALYSIS

Data Set. Electron diffraction amplitudes $|F_h|$ from frozen-hydrated two-dimensional crystals of the halorhodopsin from *Halobacterium halobium* were obtained at 120 kV to 6-Å resolution, as described by Havelka *et al.* (16). There were 101 data points in the unique set. The centrosymmetric plane group of the square projection (a = 102 Å) is p4gm (# 12) (17). A set of crystallographic phases obtained from the Fourier transform of averaged electron micrographs was also published by these authors.

Normalized structure factors $|E_h|$ were calculated from these amplitudes by using the formula: $E_h^2 = F_h^2/\varepsilon[\overline{F^2}]$, where the denominator is the mean value of intensities within a nearby shell of reciprocal space. A correction factor ε is applied to account for special classes of intensities (e.g., those lying on reciprocal axes with systematic absences).

Construction of a Basis Phase Set. In the earlier use (10) of the Sayre–Hughes equation (18), $E_h = N^{1/2} \Sigma_k E_k E_{h-k}$, it was found that a set of 20 unique reflections at 15-Å resolution (Table 1) provided a suitable starting point to extend the image-derived crystallographic phases to the electron diffraction resolution of the halorhodopsin data set. The same basis set was used for this study. From the symmetry of the plane group, it could be shown, by simplification of the trigonometric

The publication costs of this article were defrayed in part by page charge payment. This article must therefore be hereby marked "*advertisement*" in accordance with 18 U.S.C. §1734 solely to indicate this fact.

Table 1. Basis data set for halorhodopsin to 15-Å resolution

			Phase		
*hk*0	|*F*|	|*E*|	Correct	Starting	After annealing
020	245.9	1.39	π	π	π
040	8.4	0.05	π	0*	0*
060	66.7	1.56	0	π*	0
110	126.7	1.01	π	π	π
120	25.5	0.20	0	0	0
130	89.8	0.72	0	0	0
140	17.7	0.14	π	π	π
150	31.9	1.04	0	0	0
160	14.7	0.48	0	π*	π*
220	293.2	2.35	π	π	π
230	18.8	0.15	π	0*	0*
240	42.0	0.34	0	0	0
250	15.2	0.50	π	π	π
260	18.6	0.61	0	0	0
330	117.6	0.94	π	0*	π
340	18.3	0.60	0	π*	π*
350	20.0	0.65	0	π*	π*
360	35.2	1.15	0	0	0
440	17.4	0.57	π	0*	0*
450	11.7	0.38	π	π	π

*Incorrect.

form of the structure factor expression, that *hk*0 reflections with *gg*0 or *uu*0 (where *g* = "gerade" or even and *u* = "ungerade" or odd) are both structure invariants. Only the parity group $ug0 = gu0$ could be used for origin definition; e.g., for the reflections in Table 1 with highest $|E_h|$ value, the phase term $\varphi_{360} = 0$ could be specified *a priori*. Algebraic values were then assigned to four other phases of high $|E_h|$ reflections, viz: φ_{020}, φ_{110}, φ_{150}, and φ_{220}. These were permuted through $0,\pi$ to generate 16 starting phase sets, each containing 5 reflections.

The starting phase sets were then used to generate a larger set via the Sayre–Hughes equation. In this convolution of normalized structure factors, it was important that an estimate of the E_{000} term be given to stabilize the phases of the basis set. [Expansions of image-derived phase terms in earlier work (10) were made with or without this term, but, when it was not used, the basis set always had to be reset to the starting values.] Finding the exact value of E_{000} is not necessary. A suitable estimate could be made by assuming that there are 8 molecular units of approximate molecular weight 26,000 (the value for bacteriorhodopsin) in the unit cell. The E_{000} value (132.0) was then found by dividing this by the atomic weight of carbon and then taking the square root. The initial Sayre expansion of the 16 starting phase sets provided phase estimates for 17 of 20 reflections, with reasonable amplitude estimates given only for the reflections used as the basis set. From these expansions, 6 starting sets were chosen where the summed $|E_h|$ amplitude of the original 5 reflections retained a maximum value. After assigning observed $|E_h|$ values to the new phase estimates, another cycle of the Sayre equation provided phase estimates for all 20 reflections. The remaining 3 phase estimates were then associated with their $|E_h|$ values to carry out a final Sayre convolution for the six starting phase sets.

An optimal starting phase set was found from the six possible solutions by comparing observed and predicted values of $|E_h|$; i.e.,

$$D_h = \| E_h|_{\text{obs}} - |K \sum_k E_k E_{h-k} \|,$$

where K is adjusted so that $\Sigma\, |E_h|_{\text{obs}} = \Sigma\, |E_h|_{\text{calc}}$. The phase set corresponding to the minimum value of D_h contained eight errors (Table 1). The initial potential map associated with this set is shown in Fig. 1*a*.

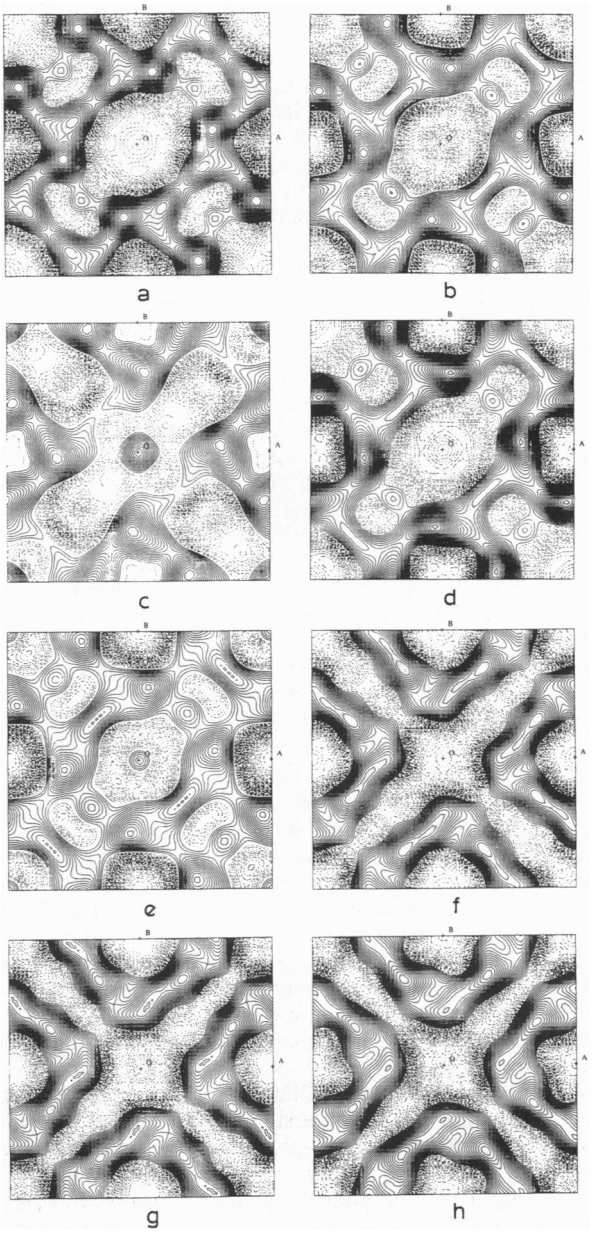

FIG. 1. Potential maps for halorhodopsin at 15-Å resolution (calculated from phased $|F_h|$ with no F_{000} term). (*a*) Starting phase set. (*b*) Change phase of (060) reflection. (*c*) Change phases of (060) and (020) reflections. (*d*) Change phases of (060) and (150) reflections. (*e*) Change phases of (060) and (110) reflections. (*f*) Change phases of (060) and (330) reflections. (*g*) Change phases of (060), (330), and (130) reflections. (*h*) Correct phase set. (See also Table 2.)

Because the most accurate basis set was necessary for a resolution expansion, the initial phase estimate had to be improved by an annealing step. This was carried out by sequentially changing the phase values for reflections with large $|E_h|$ values. Only the phase terms for the (360) and (220) reflections were assumed to be correct, the former because it was used to define the origin and the latter because it retained the same phase value for all of the six starting sets selected above. Although, initially, D_h was tried as a figure of merit for selection of appropriate new phase terms during an annealing process, it was soon found to be a weak determinant for the evaluation of individual reflections, especially since false minima were found corresponding to erroneous phase changes.

The best figure of merit for deciding whether the phase of an individual reflection should be changed was the density

flatness criterion $q = \langle \Delta\rho^4 \rangle$, originally defined by Luzzati *et al.* (19). For this evaluation, potential maps, based on F_h, were calculated, where $F_{000} = 0.0$, so that the average distribution of map pixel density ρ was constrained around a zero level. Since the computer program used to calculate the potential maps provided the upper and lower bounds of the density distributions, the selection of likely phase terms to be corrected could be made intuitively. That is to say, if a change in phase yielded a map with expanded density limits and a more "peaky" distribution of density, the change could be rejected. The selection could also be placed on the more quantitative basis of selecting for values of q, as outlined in Fig. 1 and Table 2. Hence, the phases associated with the largest $|E_h|$ terms were changed and q was evaluated to see whether the change could be justified. If there was a significant difference in this figure of merit, the new phase was accepted and another reflection with slightly lower $|E_h|$ value was sought that would again result in a noticibly lower value for q. After changing the value of the (330) and (060) phases (Table 2), a starting set was obtained with six errors but giving a map with a density distribution visually indistinguishable from that of the correct phase set (Fig. 1*h*). It is clear that the selection of new phases is only possible for large $|F_h|$ reflections, where the change had a salient impact on the appearance of the potential map.

Phase Extension. An extension to a 10-Å resolution limit (43 unique reflections) was then made based on similar principles, but now keeping the 15-Å basis set unchanged (Table 3). First the Sayre–Hughes convolution was carried out to produce an initial expanded phase set containing a total of 15 errors (6 of these in the original basis set) leading to the map in Fig. 2*a*. Sequential annealing of individual phases was then begun, evaluating the magnitude of q, as before, and in the order of decreasing $|E_h|$ values for the selected reflections. Phase changes were positively justified for the (460), (560), and (550) reflections, yielding the potential map in Fig. 2*b*. Although an additional change of phase for the (770) reflection did not produce a markedly changed q value, a more even distribution of density in the potential map (Fig. 2*c*) led to this possibility being tested in the further expansion to 6 Å. (A map calculated from the correct phase set is shown in Fig. 2*d* for comparison.)

After this intermediate resolution was reached, the Sayre–Hughes equation was used to extend the corrected 10-Å basis sets to 6 Å. At this higher resolution there were no new reflections with large enough $|F_h|$ amplitudes to justify any further annealing step. Thus the phase extension was stopped at this point. Phase errors for this *ab initio* determination are compared in Table 4 to the values obtained earlier when the image basis set was expanded. Potential maps calculated from the two final phase sets are shown in Fig. 3 *a* and *b*, where they are also compared to the solution reached earlier from image-derived phases (Fig. 3*c*). The phase set including a changed (770) phase term is thus seen to be the best solution, based on the density flatness criterion q. In terms of the phase residual defined by Unwin and Klug (20), $R(\varphi) = (\Sigma\, |F_h||\Delta\varphi^2|/\Sigma\, |F_h|)^{1/2}$, the overall error is 67.3° for all 101 data points or 56.3° for all $|F_h| \geq 10.0$. [The $|F_h|$ values listed earlier (10) were multiplied by 10.] The similarities between this solution and the structure based on image phases are quite striking.

Table 2. Sequence of annealing steps for the 15-Å basis set

Step	q	Depiction	Decision
Begin	1.65	Fig. 1*a*	
Change (060)	1.46	Fig. 1*b*	Accept change to (060)
Change (060) and (020)	1.83	Fig. 1*c*	Reject change to (020)
Change (060) and (150)	1.40	Fig. 1*d*	Difference not large, reject change to (150)
Change (060) and (110)	3.31	Fig. 1*e*	Reject change to (110)
Change (060) and (330)	1.20	Fig. 1*f*	Accept change to (330)
Change (060), (330), and (130)	2.92	Fig. 1*g*	Reject change to (130)

q = 1.23 for correct phase set.

Table 3. Expanded phase set for halorhodopsin to 10-Å resolution

			Phase		
$hk0$	$\|F\|$	$\|E\|$	Correct	Expanded	After annealing
080	98.1	2.26	π	π	π
0100	20.1	1.46	0	0	0
170	20.9	0.68	π	π	π
180	26.2	0.85	π	π	π
190	13.1	0.43	0	0	0
270	4.3	0.14	π	0*	0*
280	33.7	1.10	π	π	π
290	7.2	0.23	0	0	0
2100	48.1	4.96	0	0	0
380	11.6	0.38	π	π	π
390	15.3	0.50	π	π	π
460	50.4	1.64	0	π*	0
470	24.5	0.80	0	π*	π*
480	25.8	0.84	π	π	π
490	5.2	0.54	0	π*	π*
550	50.8	1.65	π	0*	π
560	41.5	1.35	π	0*	π
570	12.0	0.39	0	0	0
580	6.1	0.20	π	π	π
660	17.1	0.56	0	0	0
670	16.1	0.52	0	π*	π*
680	13.3	1.37	π	0*	0*
770	20.3	2.09	π	0*	0*,π

*Incorrect.

DISCUSSION

Although the phase values found in this study are not quite as accurate as those obtained from determinations based solely on electron micrographs (16), or the extension of a low-resolution set derived from such images (10), it is clear that an *ab initio* analysis of a protein structure at medium resolution will, nevertheless, lead to a useful result. From the stand point

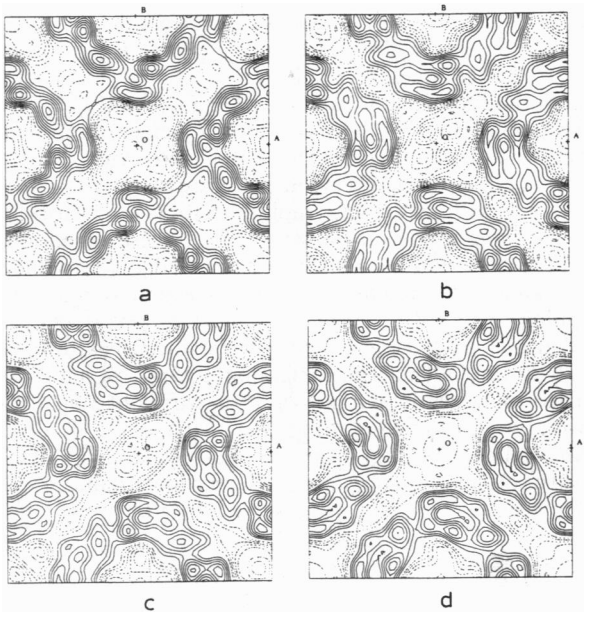

FIG. 2. Potential maps for halorhodopsin at 10-Å resolution. (*a*) Initial expanded set. (*b*) Change phases of (460), (560), and (550) reflections. (*c*) Change phases of (460), (560), (550), and (770) reflections. (*d*) Correct phase set.

Table 4. Mean phase errors $\langle|\Delta\varphi|\rangle$ for halorhodopsin

	Direct methods	Phase extension*	
		F·F	*E·E*
To 10 Å	46.0°	16.7°	16.7°
To 6 Å, all data	74.8°	60.6°	55.2°
To 6 Å, $\|F_h\| \geq 10$	44.0°	32.0°	24.0°

*Refers to Sayre convolution based on *F* or *E*.

of molecular substitution, it is clear that the map in Fig. 3*b* contains a subunit very similar to the one found for bacteriorhodopsin (8), a premise that could be justified further by correlational matching. The map itself contains a number of the projected α-helical positions found for the halorhodopsin by image analysis. It may be possible that the phase accuracy could be improved at this stage by density modification procedures (21–23). Because the goal of this study was merely to evaluate the suitability of *ab initio* direct phasing procedures, this further refinement step was not undertaken.

The most interesting aspect of this direct analysis of a medium resolution data set is just that it is feasible, given the rather pessimistic estimates found in the x-ray crystallographic literature. For example Fan *et al.* (24) have discussed how the normal Cochran criterion for finding a structure solution (i.e., finding a maximum value for the integral $\int_v \rho^3\, dV$) is not a suitable condition at low resolution when determining the

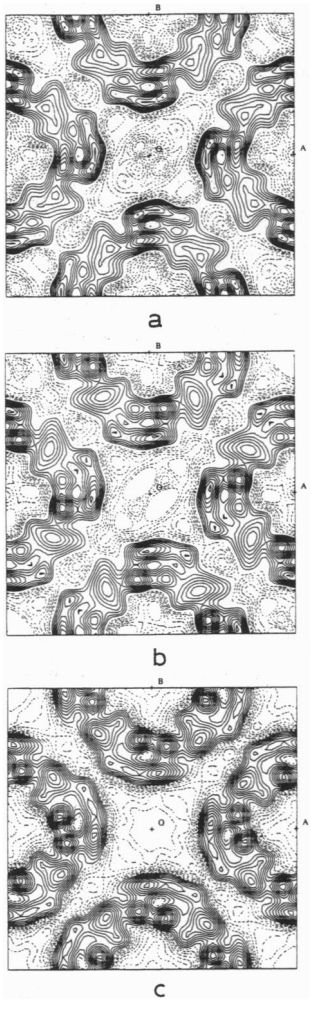

FIG. 3. Potential maps for halorhodopsin at 6 Å. (*a*) Expansion from basis set of Fig. 2*a*. (*b*) Expansion from basis set of Fig. 2*b*. (*c*) Correct phase set.

structures of proteins. On the other hand, nearly atomic-resolution determinations still conform to the Cochran criterion, even if the statistical accuracy of phase estimates generated by traditional direct methods is not particularly good. Indeed, such high-resolution phase extensions based on the Sayre equation or the tangent formula have been published (25–30). More recently, even *ab initio* determinations, based on more powerful direct phasing approaches, have been reported (12–14).

As also stated earlier by Podjarny and Yonath (30), requirements for the analysis of a macromolecular structure differ for various resolution limits. In extensive low-resolution phase expansions based on incomplete multiple isomorphous replacement phase sets, these authors (32, 33) had shown that conventional phase-extension techniques still will produce useful results, despite later criticisms of their use (30, 34). This conclusion is also borne out by the successful application of maximum entropy or Sayre convolution expansions of image-derived phase sets (9–11) to the resolution of electron diffraction patterns. Thus, the technique for generation of phases itself works equally well within confined low- and high-resolution domains and is only challenged when a "nodal" region of average intensity is encountered (e.g., near 5 Å for proteins), requiring the inclusion of branching points into the phasing tree and the evaluation of these multiple solutions by some suitable criterion (10). It is clear that the phase-extension method is most suitable when a very accurate basis phase set can be obtained (e.g., from the Fourier transform of an electron micrograph). When such information is not available, multisolution and annealing steps must be included to overcome the weakness of single-solution approaches (30) for *ab initio* phasing of protein data.

Although the methods for phase generation can be the same at low and high resolution, the criteria for selection of the best phase set, by necessity, must differ. This is precisely because the implied condition of maximum "peakiness" of the density function has no meaning at low resolution, since individual atomic positions cannot be visualized with such limited data. The Cochran figure of merit (35), therefore, might be replaced by a maximum smoothness or flatness criterion for map density, the latter recognized earlier by Luzzatti *et al.* (36) to satisfy the best maximum entropy condition for such limited resolution structures. This approach has already been shown to be effective for the *ab initio* phase determination of lipid bilayer profiles (37). An alternative test for density smoothness (i.e., the average slope of the density distribution) has also been found to be useful (37). Drawbacks in the use of such figures of merit, particularly for phase annealing, are that only suitably large changes in density distribution can be observed if the phases of individual reflections are varied sequentially. A cluster annealing of several reflections at a time may be more effective, even though this possibility was not evaluated in this study. Also, it is not yet certain just how absolutely reliable the flatness criterion is. False minima have been detected occasionally in earlier studies of lipid bilayer profiles, for example (37). However, since these earlier determinations were carried out to much higher resolution (e.g., 3.4 Å), a comparison to the present case may not be valid. Perhaps a test of more than one figure would be more useful, as it has been in the selection of best solutions in conventional multisolution approaches to solving the phase problem (38).

There are reasons to expect that other analyses of this type, including noncentrosymmetric projections, will be possible, even with the above caveats taken into account. Fan *et al.* (24) have pointed out that the low-angle intensity data from a protein are the strongest and hence the relationships between them should not be weaker on average than they would be for any other structure. Building up the best possible basis phase set at low resolution, therefore, seems to be the most important criterion for expanding to a chemically meaningful structure at

higher resolution. It appears also that the search for the flattest density profile, after the generation of multiple phase sets, is the most reasonable way to find these initial phases. (Also, in electron crystallography, it is worthwhile to consider whether a more accurate set of structure factor magnitudes collected at lower electron wavelength would help to improve the initial phase expansion.)

This research was supported by a grant from the National Institute of General Medical Sciences (GM-46733), which is gratefully acknowledged.

1. Amos, L. A., Henderson, R. & Unwin, P. N. T. (1982) *Prog. Biophys. Mol. Biol.* **39,** 183–231.
2. Glaeser, R. M. (1985) *Annu. Rev. Phys. Chem.* **36,** 243–275.
3. Jap, B. K., Zulauf, M., Scheybani, T., Hefti, A., Baumeister, W., Aebi, U. & Engel, A. (1992) *Ultramicroscopy* **46,** 45–84.
4. Henderson, R., Baldwin, J. M., Ceska, T., Zemlin, F., Beckmann, E. & Downing, K. H. (1990) *J. Mol. Biol.* **213,** 899–929.
5. Kühlbrandt, W., Wang, D. N. & Fujiyoshi, Y. (1994) *Nature (London)* **367,** 614–621.
6. Jap, B. K., Walian, P. J. & Gehring, K. (1991) *Nature (London)* **350,** 167–170.
7. Cowan, S. W., Schirmer, T., Rummel, G., Steiert, M., Ghosh, R., Pauptit, R. A., Jansonius, J. N. & Rosenbusch, J. P. (1992) *Nature (London)* **358,** 727–733.
8. Henderson, R., Baldwin, J. M., Downing, K. H., Lepault, J. & Zemlin, F. (1986) *Ultramicroscopy* **19,** 147–178.
9. Gilmore, C. J., Shankland, K. & Fryer, J. R. (1993) *Ultramicroscopy* **49,** 132–146.
10. Dorset, D. L., Kopp, S., Fryer, J. R. & Tivol, W. F. (1995) *Ultramicroscopy* **57,** 59–89.
11. Dorset, D. L. (1995) *Proc. Microsc. Soc. Am.* **53,** in press.
12. Woolfson, M. M. & Yao, J. X. (1990) *Acta Crystallogr. A* **46,** 409–413.
13. Sheldrick, G. M., Dauter, Z., Wilson, K. S., Hope, H. & Sieker, L. C. (1993) *Acta Crystallogr. D* **49,** 18–23.
14. Weeks, C. M., Hauptman, H. A., Smith, G. D., Blessing, R. H., Teeter, M. M. & Miller, R. (1995) *Acta Crystallogr. D* **51,** 33–38.
15. Urzhumtsev, A. G., Podjarny, A. D. & Navaza, J. (1994) *Joint CCP4 ESF-EACBM Newsl. Protein Crystallogr.* **30,** 29–36.
16. Havelka, W. A., Henderson, R., Heymann, J. A. W. & Oesterhelt, D. (1993) *J. Mol. Biol.* **234,** 837–846.
17. Hahn, T., ed. (1992) *International Tables for Crystallography: Vol. A. Space-Group Symmetry* (Kluwer, Dordrecht, The Netherlands), 3rd Ed.
18. Sayre, D. (1980) in *Theory and Practice of Direct Methods in Crystallography*, eds. Ladd, M. F. C. & Palmer, R. A. (Plenum, New York), pp. 271–286.
19. Luzzati, V., Tardieu, A. & Taupin, D. (1972) *J. Mol. Biol.* **64,** 269–286.
20. Unwin, P. N. T. & Klug, A. (1974) *J. Mol. Biol.* **87,** 641–656.
21. Schevitz, R. W., Podjarny, A. D., Zwick, M., Hughes, J. J. & Sigler, P. B. (1981) *Acta Crystallogr. A* **37,** 669–677.
22. Wang, B. C. (1985) *Methods Enzymol.* **115,** 90–113.
23. Zhang, K. Y. J. & Main, P. (1990) *Acta Crystallogr. A* **46,** 41–46.
24. Fan, H. F., Hao, Q. & Woolfson, M. M. (1991) *Z. Kristallogr.* **197,** 197–208.
25. Reeke, G. N., Jr., & Lipscomb, W. N. (1969) *Acta Crystallogr. B* **25,** 2614–2623.
26. Sayre, D. (1974) *Acta Crystallogr. A* **30,** 180–184.
27. Blundell, T. L., Pitts, J. E., Tickle, I. J., Wood, S. P. & Wu, C. W. (1981) *Proc. Natl. Acad. Sci. USA* **78,** 4175–4179.
28. Olthof, G. J. & Schenk, H. (1982) *Acta Crystallogr. A* **38,** 117–122.
29. Giacovazzo, C., Siliqi, D. & Spagna, R. (1994) *Acta Crystallogr. A* **50,** 609–621.
30. Woolfson, M. M. & Yao, J. X. (1988) *Acta Crystallogr. A* **44,** 410–413.
31. Podjarny, A. D. & Yonath, A. (1977) *Acta Crystallogr. A* **33,** 655–661.
32. Podjarny, A. D., Yonath, A. & Traub, W. (1976) *Acta Crystallogr. A* **32,** 281–292.
33. Podjarny, A. D., Schevitz, R. D. & Sigler, P. B. (1981) *Acta Crystallogr. A* **37,** 662–668.
34. Giacovazzo, C., Guagliardi, A., Ravelli, R. & Siliqi, D. (1994) *Z. Kristallogr.* **209,** 136–142.
35. Cochran, W. (1952) *Acta Crystallogr.* **5,** 65–67.
36. Luzzati, V., Mariani, P. & Delacroix, H. (1988) *Makromol. Chem. Macromol. Symp.* **15,** 1–17.
37. Dorset, D. L. (1991) *Biophys. J.* **60,** 1356–1365, 1366–1373.
38. Cascarano, G., Giacovazzo, C. & Guagliardi, A. (1992) *Acta Crystallogr. A* **48,** 859–865.